

Anomalous phase association of REE in ferromanganese crusts from Indian mid-oceanic ridges: evidence for large scale dispersion of hydrothermal iron

**L. Surya Prakash^{1,2*}, Durbar Ray², B. Nagender Nath², M. Satyanarayanan³,
K. A. Kamesh Raju^{1,2}, P. John Kurian¹, M. Dileep Kumar², A. Srinivas Rao¹**

¹ National Centre for Polar and Ocean Research (NCPOR), Ministry of Earth Sciences,
Vasco-da-Gama, Goa-403804, India

²CSIR- National Institute of Oceanography, Dona Paula, Goa-403004, India

³CSIR-National Geophysical Research Institute, Uppal Road, Hyderabad-500007, India

*Corresponding Author: Surya Prakash L., National Centre for Polar and Ocean Research,
Vasco-da-Gama, Goa-403804, India.

E-mail: sukumaarya@gmail.com

Abstract

Ferromanganese crusts collected at selected locations along the ~7000 km long stretch of Carlsberg, Central Indian and Southwest Indian ridges are studied for bulk geochemical composition and distribution of rare earths and yttrium in major geochemical phases; exchangeable/carbonate, Mn-oxide, Fe-oxyhydroxide and residual silicate. The crusts are dominated by vernadite with traces of quartz and calcite. A high concentrations of major (Fe, Mn), trace (Co, Ni, Cu & Zn) and rare earth elements indicates that these crusts are hydrogenous in nature. However, the negative or no cerium anomalies in the shale normalized REE pattern indicates that some of these crusts are of mixed type (hydrogenous and hydrothermal). Irrespective of their nature (mixed or hydrogenous), the phase distribution of REE-Y shows 70-83% of total REE-Y are associated with Fe-oxyhydroxide phase, whereas only about 17-30% are associated with Mn-oxide phase. Such phase-distribution is expected in mixed type crusts because it is a combination of hydrothermal (where 90% of the total REE-Y is associated with only Fe-oxyhydroxide phase) and hydrogenous processes (where 50% of the total REE-Y is associated with only Fe-oxyhydroxide phase). Conversely, the hydrogenous crusts also shows similar phase-distributions (70-83% association with Fe-oxyhydroxide phase) which is certainly different from typical hydrogenous crusts where both Fe-oxyhydroxide and Mn-oxide phases host equal amounts (50% each). The large scale dispersion of hydrothermal particulate iron along the Indian Ocean ridges is likely to contribute an additional Fe-bound REE-Y pool to these crusts. The positive yttrium anomaly in Mn-oxide phase of all these crusts substantiates the hydrothermal contribution.

Key words: Indian mid-oceanic ridges, hydrothermal iron, hydrogenous ferromanganese crust, REE distribution, Yttrium

1 Introduction

Hydrothermal fluids emitting from active vents carry various chemical components of magmatic origin to deep ocean and cause significant compositional changes to seawater (Lang, 2018). Iron and rare earths are abundant in these fluids (Michard, 1989; Klinkhammer et al., 1994; Douville et al., 1999) (when compared with the background seawater) and co-precipitate during mixing with seawater (German et al., 1990). In the buoyant stage of hydrothermal fluid, anhydrite scavenges the rare earths (Chavagnac et al., 2018) and then in the neutrally buoyant stage, iron oxy-hydroxides scavenge rare earths from the seawater (German et al., 1990). Hence, the rare earth element concentrations are very low in hydrothermal plume particles (Mitra et al., 1994; Sherrell et al., 1999) and the hydrothermal ferromanganese crusts (Mills et al., 2001). On the other hand, hydrogenous ferromanganese crusts precipitated from seawater are rich in rare earth elements concentrations (Nath et al., 1997; Surya Prakash et al., 2012; Hein et al., 2016). However concentrations of these elements are relatively low in mixed type crusts (hydrogenous crusts which were under influence of hydrothermal activity (Nath et al., 1997; Kuhn et al., 1998; Kalangutkar et al., 2015) and the pure hydrothermal crusts show a large Fe-Mn fractionation (Hein et al., 1997; Nath et al., 1997). Mineralogically, Mn-oxides in hydrogenetic crusts are essentially Fe-vernadite and birnessite and hydrothermal crusts show the presence of todorokite, asbolane and busserite (Marino et al., 2019 and references therein). The sequential leaching of hydrothermal ferromanganese crusts shows that REE are mainly associated with only Fe-oxyhydroxides (Surya Prakash et al., 2012) and for hydrogenous crusts, rare earths are associated with both Fe-oxyhydroxide (~ 50%) and Mn-oxide (~50%) in nearly same proportion (Surya Prakash et al., 2012; Ren et al., 2018).

Recent GEOTRACES studies show the mid-oceanic ridges as primary source of hydrothermal iron (Wu et al., 2011; Klunder et al., 2011, 2012; Noble et al., 2012; Thi Dieu Vu and Sohrin, 2013; Nishioka et al., 2013; Fitzsimmons et al., 2014, 2015; Resing et al., 2015; German et al., 2016; Chinni et al., 2019) and about 90% of it precipitates as Fe-oxyhydroxide near the ridges (Fitzsimmons et al., 2017). Such precipitation of particulate iron in the water column should have important implications in cycling of particle reactive elements such as rare earths in the seawater (German et al., 1990). Therefore, the signatures of large scale precipitation of hydrothermal iron and related scavenging effects are expected to be preserved in chemical precipitates such as oceanic ferromanganese crusts. Thus, we have carried out geochemical fractionation studies of several ferromanganese crusts collected at selected locations along the ~7000 km long stretch of Carlsberg, Central Indian and Southwest Indian Ridges, Indian Ocean (Figure 1 and Table 1) for assessing the association of REE-

Y with competing geochemical phases and to understand the role of hydrothermal particulate iron on the behavior of particle reactive elements in the ocean.

2 Geological setting

The Indian Ocean has four active ridges with slow, intermediate and ultra-slow active spreading ridges, namely, Carlsberg Ridge (CR), Central Indian Ridge (CIR), Southeast Indian Ridge (SEIR) and Southwest Indian Ridge (SWIR) which are part of world mid-ocean ridge system (Figure 1). The MOR section between the Owen fracture zone near 10°N and equator is named as Carlsberg Ridge. The Central Indian Ridge extends from the equator to Rodriguez Triple Junction (RTJ) at 25°S. The SWIR extends from the RTJ to the Bouvet Triple Junction (BTJ) at 55° S whereas the SEIR extends from the same RTJ to Macquarie Triple Junctions (MTJ) at 60° S. Both CR and CIR are defined as slow-spreading ridges with slightly variable rates of 22-32 mm/yr and 26-36 mm/yr respectively (Kamesh Raju et al., 2012b, 2008), while SEIR is characterized with intermediate spreading rate of 59-75 mm/yr (Small et al., 1999). However, SWIR is classified as an ultra-slow spreading ridge with a spreading rate of ~14 mm/yr (Cannat et al., 2008).

Seabed sampling of along these ridges recovered variety of basalts (glass cover, pillow, ropy, columnar, altered, oxide encrusted), coarse grained gabbros, serpentinized peridotites, gabbros and volcanic breccias (Cannat et al., 2008; Kamesh Raju et al., 2008, 2012b). Thin coating of ferromanganese oxides were recovered from majority of these rock samples. The sample locations of the present study areas (CR, CIR & SWIR) in Indian Ocean along with the active/inactive and inferred hydrothermal vents (Beaulieu et al., 2013) are shown in Figure 1.

3 Material and methods

For the present study, 24 ferromanganese crust samples were collected from Indian Ocean mid-oceanic ridge system (Figure 1 and Table 1). Among these only five samples were collected from the vicinity of reported hydrothermal plumes (Srinivasan et al., 2004; Murton et al., 2006; Ray et al., 2008, 2012; Thi Dieu Vu and Sohrin, 2013; Nishioka et al., 2013; Ray et al., 2017; Takahata et al., 2018) while the rest were away from any reported active/extinct sites.

Initially, all samples were thoroughly cleaned, air dried and then finely powdered by using agate motor and pestle. The fine powdered samples were analyzed for mineralogical composition using Rigaku X-ray diffractometer with Dmax-1c wide angle goniometer. Each sample was scanned from 05° to 85° 2θ by using Cu-Kα radiation. Minerals were identified using Rigaku standard data processing and peak search- software and the website (www.webmineral.com).

All the crust samples were investigated for bulk chemical composition and relative distribution of rare earth elements and yttrium (REE-Y) in major geochemical phases. For bulk analysis, 50 mg of each powdered crust samples were digested with supra-pure acid mixture (HF:HNO₃:HClO₄=7:3:1) for chemical disintegration described in Balaram and Rao (2003). Four major geochemical phases viz., 1) easily exchangeable/loosely adsorbed fraction, 2) easily reducible Mn-oxide fraction, 3) moderately reducible Fe-oxyhydroxide fraction and 4) residual alumina/silicate fraction were separated by sequential leaching method described in Koschinsky and Halbach (1995); Koschinsky and Hein (2003); Bau and Koschinsky (2009); Surya Prakash et al. (2012). All the sample preparations were carried out in class 10000 clean room, and class 1000 laminar flow hoods.

The bulk and leached sample solutions were analyzed for trace and REE-Y with a Quadrupole ICP-MS (Perkin-Elmer SCIEX ELAN[®] DRC-II and Agilent[®] 7700) at CSIR-National Geophysical Research Institute, Hyderabad and National Centre for Polar and Ocean Research, Goa using ¹⁰³Rh solution (20 ng/ml) as the internal standard (Balaram and Rao, 2003). Iron and manganese concentrations were measured by using Atomic Absorption Spectrometer (Perkin Elmer AAnalyst[®] 200) at CSIR-National Institute of Oceanography, Goa. Four geochemical standards MAG-1, Nod A1, Nod P1 (obtained from USGS) and JMn-1 (obtained from GSJ) were analyzed to check the analytical accuracy, which was 2% and the precision was better than ±5%. Recovery of leaching experiments was calculated as the sum of four leached concentrations divided by bulk concentrations. Excellent recoveries of 92-109 % for REE-Y were achieved and they are within the acceptable limits 86-114% (Surya Prakash et al., 2012).

4 Results and Discussion

4.1 Mineralogy and bulk geochemical composition: assessing the nature of the crusts

All ferromanganese crusts from Indian mid-oceanic ridges have poorly crystalline vernadite (δ -MnO₂) with traces of quartz, feldspar and calcite and indicate the hydrogenous nature. Diagenesis would not have influenced these crusts, as they are not in contact with sedimentary pore fluids. Moreover, absence of manganese minerals such as todorokite, asbolane and buserrite, which have been considered to be indicative of diagenetic source (Marino et al., 2018, 2019) in these crusts, further confirms the hydrogenetic nature. In most of the samples the concentrations of Fe (15-26%) was considerably higher than Mn (6-17%) and that corresponds to low Mn/Fe ratio. The concentrations of Fe, Mn and other trace/high field strength elements, and the plots of conventional ternary diagrams (Figure 2, Table 2) clearly show that most of the crusts studied here are of

hydrogenous in nature. However, few crusts fall on the boundary of line defining hydrothermal-hydrogenous field indicating the possible influence of hydrothermal activity.

The total rare earths (Σ REE) concentrations in these crusts range between 818 and 1925 ppm (Table 2) and are comparable to those found in typical hydrogenous ferromanganese deposits of the global oceans (Nath et al., 1992,1997; Hein et al., 1997; Kuhn et al., 1998; Kalangutkar et al., 2015; Hein et al., 2016; Marino et al., 2017). Such high bulk REE concentrations suggest that these crusts would have grown slowly and scavenge REE-Y from seawater over long periods of time (Bau et al., 1996). In the shale (PAAS- Post-Archean Australian Shale; McLennan, 1989) normalized REE-Y patterns most of the samples show either positive or no cerium anomalies (Figure 3, Table 2). Generally, removal of cerium from the oceanic water column through oxidative precipitation (Bau and Koschinsky, 2009) causes the positive Ce anomaly in hydrogenous crusts. However, negative cerium or no cerium anomalies in the bulk crusts indicates the influence of hydrothermal plumes (Nath et al., 1997; Kuhn et al., 1998). The observed behavior of redox-sensitive cerium is in conformity with its genetic origins, as the extent of positive cerium anomaly decreases with increase in growth rates (Takahashi et al., 2007). Further, crusts of the present study clearly fall in the mixed (hydrogenous-hydrothermal) and hydrogenous fields (Bau et al., 2014; Hein et al., 2016) in REE based discrimination plots (Figure 4). The calculated 'excess' Ce (Kuhn et al., 1998) allowed us to distinguish between the Ce(III) and Ce(IV) uptake by crusts from the seawater. In hydrothermal crusts and plume particles, Ce behaves like its trivalent neighbors REEs and exist as Ce(III). Hence the Ce_{xs}/Ce_{bulk} would be zero and suggests that there was no oxidative Ce uptake. Otherwise, in hydrogenous crusts, the Ce_{xs}/Ce_{bulk} is equal to unity where Ce is usually present as Ce(IV). However in mixed origin crusts, the Ce_{xs}/Ce_{bulk} ratio would be less than unity with slightly high Ce concentration (Figure 5) which indicates the influence of hydrothermal activity.

Thus while the mineralogy and bulk geochemical composition of all ferromanganese crusts from Indian mid-oceanic ridges are indicating their hydrogenous nature; the Ce geochemistry and REE based discrimination plots provide the evidence of hydrothermal influence on some of these crusts and thus can be defined as mixed type (hydrogenous/hydrothermal).

4.2 Anomalous phase distribution of REE-Y in crusts: constraints on possible role of hydrothermal iron

Irrespective of their origin (hydrogenous or mixed type), the relative abundances of REE-Y in four geochemical fractions of all ferromanganese crusts (Figure 6) show that about 95% of total REE-Y is associated with Fe-oxyhydroxides (here after named as Fe-fraction) and Mn-oxide (here after named

as Mn-fraction). Among these two oxide fractions, Fe-fraction hosts about 70-83% of total REE-Y (Figure 6a, 6b & 6c) while Mn-fraction hosts only 17-30% of total REE-Y. Such REE-Y distributions in these crusts from the mid-oceanic ridges is quite contrasting to typical hydrogenous crusts of Indian Ocean (Surya Prakash et al., 2012), where both Fe-oxyhydroxide and Mn-oxide phases share almost equal amounts (45-50%) of total REE-Y (Figure 6d & 6e). In seawater, the Mn-oxide and Fe-oxyhydroxide particles develop negative and positive surface charges (Koschinsky and Halbach, 1995; Koschinsky and Hein, 2003) and thus preferentially adsorb dissolved mono- and di-carbonate complexes of REE-Y respectively (Byrne, 2002). The same mechanism based on electrostatic attraction is responsible for equal distribution of REE in hydrogenous crusts (Surya Prakash et al., 2012). However, the observed REE-Y enrichment in Fe-fraction of crusts from mid-oceanic ridges resembles typical hydrothermal crusts from Andaman Sea (Figure 6f) and could not be explained with similar scavenging mechanism as described for hydrogenous crusts. In hydrothermal crusts, the uptake of dissolved REE by hydrothermal particles has been explained in terms of co-precipitation with iron in addition to adsorption mediated by columbic attraction. Further, the dominant negatively charged or neutral halide/sulphate species of dissolved REE in hydrothermal fluids preferentially adsorbed on Fe-oxyhydroxides and leave the Mn-oxide phase poor in REE (Surya Prakash et al., 2012). Therefore, the REE-Y distributions of mixed origin crusts with 70% REE in Fe-fractions (Figure 6a, 6b, 6c) appear to be the intermediate member of pure hydrothermal (90% of the total REE are associated with Fe-fraction) and hydrogenous (~50% of the total REE are associated with Fe-fraction) origin. Therefore, even if the high concentrations of REE in the crusts from mid-oceanic ridges are comparable to other hydrogenous crusts; relative enrichment of REE-Y in Fe-fraction suggest that a substantial fraction of the total REE is probably contributed by Fe-particles from hydrothermal sources(s).

4.3 Yttrium anomaly in REE-Y pattern: evidence for hydrothermal contribution

Like phase distribution of REE-Y; certain features in PAAS-normalized REE-Y patterns of sequentially leached fractions (Figure 7A-7E) of crusts from mid-oceanic ridges also differ from hydrogenous crusts. In bulk REE patterns, the crusts are characterized with distinct positive Ce-anomalies; very similar to those found in hydrogenous deposits from Indian Ocean (Figure 7F & 7G). However, the positive cerium anomalies in both Mn-oxide ($Ce/Ce^* = 1.32-1.88$) and Fe-oxyhydroxide phases ($Ce/Ce^* = 1.84-2.47$, Supplementary Material) of the crusts from mid-oceanic ridges are comparable to hydrogenous crusts from Indian Ocean. These cerium anomalies result from oxidation of dissolved Ce(III) after its sorption on surface of metal-oxide (Bau and Koschinsky, 2009). On the other hand, the mixed type crusts, unlike hydrogenous crusts, show slightly negative

or no Ce-anomalies in both Mn-oxide and Fe-oxyhydroxide fractions. Such relative depletion of Ce is in agreement with that of hydrothermal crusts from Andaman Sea (Surya Prakash et al., 2012) which further substantiates the contribution from hydrothermal sources to these crusts.

The PAAS normalized bulk REE patterns of crusts from mid-oceanic ridges show depletion of Y when compared to adjacent elements (Dy and Ho); very similar to those found in hydrogenous crusts from Indian Ocean. However, the relative enrichment of Y in Mn-oxide phase of crusts in the present study (both hydrogenous and mixed type) is in contrast to other hydrogenous crusts (Figure 7F-7G). In hydrogenous crusts, Y exhibit negative anomalies because of weak surface complexation of Y; that does not favor its adsorption on particles (Bau and Koschinsky, 2009). Thus the positive yttrium anomalies (Figure 7A-7E) in the Mn-oxide phase of crusts from CR, CIR and SWIR manifest the possible contribution from hydrothermal source ; which usually contain free Y-ion and/or its halide complexes (Bau and Dulski, 1999) and are adsorbed on Mn-oxide phase in hydrothermal crusts (Surya Prakash et al., 2012; Mikhailik et al., 2017;). Therefore, these positively charged Y-ion/complexes would preferentially adsorb onto Mn-oxide and might be responsible for positive anomalies (Figure 7). The shale normalized Y/Ho ratios in the Mn-oxide phase of the crusts (average of all samples) from mid-oceanic ridges is 1.2 (Supplementary Information); which further substantiate the hydrothermal origin of Y. This ratio (above 1.0) is quite close to those $(Y/Ho)_{SN}$ of hydrothermal crusts (2.14- average) but distinctly different from the hydrogenous crusts (0.85-average and less than 1) from the Indian Ocean (Surya Prakash et al., 2012).

Moreover, irrespective of sampling locations along the mid-oceanic ridge, the similar features of REE-distribution in geochemical phases of all the crusts suggest a pervasive supply of hydrothermal-Fe all along these mid-oceanic ridges. Although the present day hydrothermal activity is not evident all along the Indian Ocean mid-oceanic ridges, the observed hydrothermal signature in these ferromanganese crusts clearly suggest the contribution of hydrothermal iron. Earlier it was assumed that the dissolved Fe from hydrothermal vents precipitate as oxide or oxy-hydroxide with-in few kilometers of any active vent (Field and Sherrell, 2000). However, several recent studies showed that hydrothermal-Fe travels further away from its source as organic complexes (Toner et al., 2009; Sander and Koschinsky, 2011) and/or pyrite nano-particles (Yücel et al., 2011). Further, Fitzsimmons et al. (2017) have traced the hydrothermal particulate-Fe as far as 4300 km away from the active source. Thus, it is evident from these recent studies, that the hydrothermal-Fe is transported thousands of kilometers in the deep oceans. Therefore, even if ~90% of the hydrothermal-Fe precipitates very close to their sources, a considerable amount of Fe and associated

REE seems to move further and precipitate away from the source and these signatures are retained in hydrogenous crusts collected all along the mid-oceanic ridges.

4.4 Proposed mechanism for formation of crusts at mid-oceanic ridges

In normal oceanic water column, below the oxygen minimum zone (OMZ), dissolved iron and manganese get oxidized and forms colloids (Koschinsky and Halbach, 1995). These colloidal particles of Mn and Fe oxides develop surface charge and adsorb charged species of other elements available in seawater. Since the zero point charge for Mn-oxide (pH_{ZPC}) is 2.8 and 8.5 for $\text{Fe}(\text{OH})_3$ (Stumm and Morgan, 1981); in seawater (pH is 7.8) the surface of Mn-oxides develop negative charge in seawater and attracts the positively charged mono-carbonate complexes of rare earths i.e., $\text{REE}(\text{CO}_3)^+$ (Byrne, 2002). On the other hand, the surface of $\text{Fe}(\text{OH})_3$ would develop positive charge and attracts the negatively charged di-carbonate complexes of rare earth elements ($\text{REE}(\text{CO}_3)_2^-$). Thus, the charge-based scavenging mechanism (electrostatic attraction of these particles (Koeppenkastrop and De Carlo, 1992) promotes nearly equal share (~50%) of REEs among Mn-oxide and Fe-oxyhydroxide colloids in pure hydrogenous crusts (Surya Prakash et al., 2012; Ren et al., 2018). In contrast, during hydrothermal precipitation, both REE and Fe are (co)precipitated from the hydrothermal fluid and almost 90% REE are associated with Fe-oxyhydroxides (Surya Prakash et al., 2012). However, the present study has shown that in the crusts collected from mid-ocean ridges, such distribution of REE-Y in two oxide fractions are intermediate of pure hydrogenous/hydrothermal crusts. To explain such anomalous REE distributions, here we propose a mechanism of formation of ferromanganese crusts at the mid-oceanic ridges (Figure 8). After the redox-driven precipitation from the subsurface reactions at the base of OMZ (around 1500m), hydrothermal input in the mid- to deep- water column (2000-4000m approximately) is possible. When the Mn and Fe oxides are formed at the OMZ boundary, they possibly adsorb near equal amounts of carbonate complexes of REE-Y from the seawater (as evidenced by 50% REE-Y each in Mn and Fe-oxides in hydrogenous crusts). When these particles sink through the hydrothermal plume layers, they acquire the hydrothermal iron-oxyhydroxide which hosts 90% REE by co-precipitation and also decoupled (Fitzsimmons et al., 2017) with Mn-oxide in the plume layer. Therefore, the resultant Fe-Mn oxide precipitate (crusts here) will have maximum REE associated with Fe-oxyhydroxide (70-80%) with relatively less REE association with Mn-oxide (20-30%). Therefore, at mid-oceanic ridges, high abundance of hydrothermal particulate iron oxyhydroxides serves as “an additional scavenger” for dissolved REE in seawater, similar to that of other particles reactive elements such as thorium (Valk et al., 2018; Pavia et al., 2019) and can become a part of authigenic sinks such as crusts.

5 Implication of the present study

The results of sequential leaching experiment on ferromanganese crusts from the Indian mid-oceanic ridges indicate that hydrothermal Fe-oxyhydroxides transporting over a large distance can contribute to the chemistry of ferromanganese crusts all along the ridges. Like previous results of international GEOTRACES program; showing extensive spreading of hydrothermal-Fe in Indian Ocean (Nishioka et al., 2013), here our observations also confirm widespread chemical precipitation of hydrothermal iron along the ridges. The ferromanganese crusts from other oceanic ridges may have similar pattern as large scale dispersion of hydrothermal-Fe plumes have been reported in the global oceans too. Therefore, while discussing the geochemistry of authigenic fractions of crusts/sediments from mid-oceanic ridges, one may consider possible hydrothermal contribution. Although numerous studies have shown wide spread hydrothermal iron along the Indian ridges, the dynamical mechanism for its transportation is not clearly defined. But when we consider the cross-ridge similarities of SWIR and CIR hydrothermal vent biodiversity (Sun et al., 2020), there is possible extension of intra-ridge deep water connectivity from south to north along the Indian ridge system. This is in agreement with our understanding that the general flow of bottom waters (such as Antarctica Bottom Water and North Atlantic Deep Water) in the western Indian Ocean is from south to north (Kumar and Li, 1996; Wilson et al., 2012) which is obstructed by ridges and plateaus, but passing through openings and fracture zones.

6 Conclusions

The ferromanganese crusts at several locations all along the ~7000 km long transect of Indian mid-ocean ridges have vernadite as major mineral along with minor quartz and calcite and high concentrations of Fe, Mn and total REE, similar to hydrogenous crusts. However the shale normalized REE pattern of some of these crusts shows the negative or no cerium anomalies which indicates the influence of hydrothermal activity. Irrespective of their origin, the significant percent of total REE-Y were found to preferentially associate with Fe-oxyhydroxide phase in contrast to typical hydrogenous crusts. The high abundance of REE-Y in Fe-oxyhydroxide phase reflects the hydrothermal iron contribution to the total REE in all these samples irrespective of their locations along the mid-oceanic ridge system. The positive Y anomaly in the Mn-oxide phase further substantiates the evidence of hydrothermal inputs in these crusts. However, due to masking effects of major hydrogenous components, the evidences of hydrothermal contributions are not prominent in bulk geochemistry. Therefore, beside the adsorption mechanism which usually concentrates REE-Y in hydrogenous crust from seawater, possibly, hydrothermal Fe particulates and associated REE also partially contribute to the total REE of the crusts from the mid-oceanic ridges. Thus, the results of

this study provide additional evidence for widespread distribution of hydrothermal iron in deep waters along the Indian mid-oceanic ridges.

Acknowledgement

We thank the Directors of NCPOR, Ministry of Earth Sciences; CSIR-NIO, Goa and CSIR-NGRI, Hyderabad for their support and encouragement. Thanks to Dr. Mudholkar for providing crust samples collected from Central Indian Ridge. Thanks to Drs. Thamban, and Rahaman, Mrs. Lathika, Ms. Ankita, Mr. Taarique of NCPOR and Dr. Sawant of NGRI, for their help in ICPMS analysis. We thank Girish Prabhu, NIO for XRD analysis. This work was carried out as a part of the Indian Ridge program (Grant no. 30-(2050)/COR06/2003-Finance, CSIR and Grant no. MoES/Hydro-Sulphides/04/08-PC-II) and Hydrothermal Sulphides program (Grant no. MOES/EFC/28/2018-II) funded by the Ministry of Earth Sciences, Govt. of India. We acknowledge the masters, crew members, scientific and technical colleagues onboard ORV Sagar Kanya, RV Sonne, MV Boris Petrov and Akademik Strakov for their support during the cruises. LSP thanks, CSIR, India for Senior Research Fellowship (Grant No.: 31/26(186)/2010-EMR-I) and samples from Carlsberg and Central Indian Ridges are part of my doctoral thesis. We are thankful to the editor and two anonymous reviewers for their constructive comments on the manuscript. This is NCPOR contribution no. XXXX and NIO contribution no. XXXX.

References

- Balaram, V., Rao, T.G., 2003. Rapid Determination of REEs and Other Trace Elements in Geological Samples by Microwave Acid Digestion and ICP-MS. *At. Spectrosc.* 24, 206–212.
- Bau, M., Dulski, P., 1999. Comparing yttrium and rare earths in hydrothermal fluids from the Mid-Atlantic Ridge: Implications for Y and REE behaviour during near-vent mixing and for the Y/Ho ratio of proterozoic seawater. *Chem. Geol.* 155, 77–90. [https://doi.org/10.1016/S0009-2541\(98\)00142-9](https://doi.org/10.1016/S0009-2541(98)00142-9)
- Bau, M., Koschinsky, A., 2009. Oxidative scavenging of cerium on hydrous Fe oxide: Evidence from the distribution of rare earth elements and yttrium between Fe oxides and Mn oxides in hydrogenetic ferromanganese crusts. *Geochem. J.* 43, 37–47. <https://doi.org/10.2343/geochemj.1.0005>
- Bau, M., Koschinsky, A., Dulski, P., Hein, J.R., Universitt, F., Park, M., Bau, M., Koschinsky, A., Dulski, P., Hein, J.R., 1996. Comparison of the partitioning behaviours of yttrium, rare earth elements, and titanium between hydrogenetic marine ferromanganese crusts and seawater. *Geochim. Cosmochim. Acta* 60, 1709–1725. [https://doi.org/10.1016/0016-7037\(96\)00063-4](https://doi.org/10.1016/0016-7037(96)00063-4)
- Bau, M., Schmidt, K., Koschinsky, A., Hein, J., Kuhn, T., Usui, A., 2014. Discriminating between different genetic types of marine ferro-manganese crusts and nodules based on rare earth elements and yttrium. *Chem. Geol.* 381, 1–9. <https://doi.org/10.1016/j.chemgeo.2014.05.004>
- Beaulieu, S.E., Baker, E.T., German, C.R., Maffei, A., 2013. An authoritative global database for active submarine hydrothermal vent fields. *Geochemistry, Geophys. Geosystems* 14, 4892–4905. <https://doi.org/10.1002/2013GC004998>
- Byrne, R.H., 2002. Inorganic speciation of dissolved elements in seawater: The influence of pH on concentration ratios. *Geochem. Trans.* 3. <https://doi.org/10.1039/b109732f>
- Cannat, M., Sauter, D., Bezos, A., Meyzen, C., Humler, E., Le Rigoleur, M., 2008. Spreading rate, spreading obliquity, and melt supply at the ultraslow spreading Southwest Indian Ridge. *Geochemistry, Geophys. Geosystems* 9, Q04002. <https://doi.org/10.1029/2007GC001676>
- Chavagnac, V., Saleban Ali, H., Jeandel, C., Leleu, T., Destrigneville, C., Castillo, A., Cotte, L., Waeles, M., Cathalot, C., Laes-Huon, A., Pelleter, E., Nonnotte, P., Sarradin, P.M., Cannat, M., 2018. Sulfate minerals control dissolved rare earth element flux and Nd isotope signature of buoyant hydrothermal plume (EMSO-Azores, 37°N Mid-Atlantic Ridge). *Chem. Geol.* 499, 111–125. <https://doi.org/10.1016/j.chemgeo.2018.09.021>
- Chinni, V., Singh, S.K., Bhushan, R., Rengarajan, R., Sarma, V.V.S.S., 2019. Spatial variability in dissolved iron concentrations in the marginal and open waters of the Indian Ocean. *Mar. Chem.* 208, 11–28. <https://doi.org/10.1016/j.marchem.2018.11.007>
- Douville, E., Bienvu, P., Charlou, J.L., Donval, J.P., Fouquet, Y., Appriou, P., Gamo, T., 1999. Yttrium and rare earth elements in fluids from various deep-sea hydrothermal systems. *Geochim. Cosmochim. Acta* 63, 627–643. [https://doi.org/10.1016/S0016-7037\(99\)00024-1](https://doi.org/10.1016/S0016-7037(99)00024-1)
- Field, M.P., Sherrell, R.M., 2000. Dissolved and particulate Fe in a hydrothermal plume at 9°45'N, East Pacific Rise: Slow Fe (II) oxidation kinetics in Pacific plumes. *Geochim. Cosmochim.*

Acta 64, 619–628. [https://doi.org/10.1016/S0016-7037\(99\)00333-6](https://doi.org/10.1016/S0016-7037(99)00333-6)

- Fitzsimmons, J.N., Boyle, E.A., Jenkins, W.J., 2014. Distal transport of dissolved hydrothermal iron in the deep South Pacific Ocean. *Proc. Natl. Acad. Sci.* 111, 16654–16661. <https://doi.org/10.1073/pnas.1418778111>
- Fitzsimmons, J.N., Carrasco, G.G., Wu, J., Roshan, S., Hatta, M., Measures, C.I., Conway, T.M., John, S.G., Boyle, E.A., 2015. Partitioning of dissolved iron and iron isotopes into soluble and colloidal phases along the GA03 GEOTRACES North Atlantic Transect. *Deep. Res. Part II Top. Stud. Oceanogr.* 116, 130–151. <https://doi.org/10.1016/j.dsr2.2014.11.014>
- Fitzsimmons, J.N., John, S.G., Marsay, C.M., Hoffman, C.L., Nicholas, S.L., Toner, B.M., German, C.R., Sherrell, R.M., 2017. Iron persistence in a distal hydrothermal plume supported by dissolved-particulate exchange. *Nat. Geosci.* 10, 195–201. <https://doi.org/10.1038/ngeo2900>
- Frank, M., Marbler, H., Koschinsky, A., Van De Fliedert, T., Klemm, V., Gutjahr, M., Halliday, A.N., Kubik, P.W., Halbach, P., 2006. Submarine hydrothermal venting related to volcanism in the Lesser Antilles: Evidence from ferromanganese precipitates. *Geochemistry, Geophys. Geosystems* 7, Q04010. <https://doi.org/10.1029/2005GC001140>
- German, C.R., Casciotti, K.A., Dutay, J.C., Heimbürger, L.E., Jenkins, W.J., Measures, C.I., Mills, R.A., Obata, H., Schlitzer, R., Tagliabue, A., Turner, D.R., Whitby, H., 2016. Hydrothermal impacts on trace element and isotope ocean biogeochemistry. *Philos. Trans. R. Soc. A Math. Phys. Eng. Sci.* 374. <https://doi.org/10.1098/rsta.2016.0035>
- German, C.R., Klinkhammer, G.P., Edmond, J.M., Mura, A., Elderfield, H., 1990. Hydrothermal scavenging of rare-earth elements in the ocean. *Nature* 345, 516–518. <https://doi.org/10.1038/345516a0>
- Hein, J.R., Conrad, T., Mizell, K., Banakar, V.K., Frey, F.A., Sager, W.W., 2016. Controls on ferromanganese crust composition and reconnaissance resource potential, Ninetyeast Ridge, Indian Ocean. *Deep. Res. Part I Oceanogr. Res. Pap.* 110, 1–19. <https://doi.org/10.1016/j.dsr.2015.11.006>
- Hein, J.R., Koschinsky, A., Halbach, P., Manheim, F.T., Bau, M., Kang, J.K., Lubick, N., 1997. Iron and manganese oxide mineralization in the Pacific. *Geol. Soc. Spec. Publ.* 119, 123–138. <https://doi.org/10.1144/GSL.SP.1997.119.01.09>
- Josso, P., Pelleter, E., Pourret, O., Fouquet, Y., Etoubleau, J., Cheron, S., Bollinger, C., 2017. A new discrimination scheme for oceanic ferromanganese deposits using high field strength and rare earth elements. *Ore Geol. Rev.* 87, 3–15. <https://doi.org/10.1016/j.oregeorev.2016.09.003>
- Kalangutkar, N.G., Iyer, S.D., Mascarenhas-Pereira, M.B.L., Nath, B.N., 2015. Hydrothermal signature in ferromanganese oxide coatings on pumice from the Central Indian Ocean Basin. *Geo-Marine Lett.* 35, 221–235. <https://doi.org/10.1007/s00367-015-0402-x>
- Kamesh Raju, K.A., Chaubey, A.K., Amarnath, D., Mudholkar, A., 2008. Morphotectonics of the Carlsberg Ridge between 62°20' and 66°20'E, northwest Indian Ocean. *Mar. Geol.* 252, 120–128. <https://doi.org/10.1016/j.margeo.2008.03.016>
- Kamesh Raju, K.A., Ray, D., Mudholkar, A., Murty, G.P.S., Gahalaut, V.K., Samudrala, K., Paropkari, A.L., Ramachandran, R., Surya Prakash, L., 2012a. Tectonic and volcanic

implications of a cratered seamount off Nicobar Island, Andaman Sea. *J. Asian Earth Sci.* 56, 42–53. <https://doi.org/10.1016/j.jseaes.2012.04.018>

Kamesh Raju, K.A., Samudrala, K., Drolia, R.K., Amarnath, D., Ramachandran, R., Mudholkar, A., 2012b. Segmentation and morphology of the Central Indian Ridge between 3°S and 11°S, Indian Ocean. *Tectonophysics* 554–557, 114–126. <https://doi.org/10.1016/j.tecto.2012.06.001>

Klinkhammer, G.P., Elderfield, H., Edmond, J.M., Mitra, A., 1994. Geochemical implications of rare earth element patterns in hydrothermal fluids from mid-ocean ridges. *Geochim. Cosmochim. Acta* 58, 5105–5113. [https://doi.org/10.1016/0016-7037\(94\)90297-6](https://doi.org/10.1016/0016-7037(94)90297-6)

Klunder, M.B., Laan, P., Middag, R., De Baar, H.J.W., Bakker, K., 2012. Dissolved iron in the Arctic Ocean: Important role of hydrothermal sources, shelf input and scavenging removal. *J. Geophys. Res. Ocean.* 117. <https://doi.org/10.1029/2011JC007135>

Klunder, M.B., Laan, P., Middag, R., De Baar, H.J.W., van Ooijen, J.C., 2011. Dissolved iron in the Southern Ocean (Atlantic sector). *Deep. Res. Part II Top. Stud. Oceanogr.* 58, 2678–2694. <https://doi.org/10.1016/j.dsr2.2010.10.042>

Koepfenkastrof, D., De Carlo, E.H., 1992. Sorption of rare-earth elements from seawater onto synthetic mineral particles: An experimental approach. *Chem. Geol.* 95, 251–263. [https://doi.org/10.1016/0009-2541\(92\)90015-W](https://doi.org/10.1016/0009-2541(92)90015-W)

Koschinsky, A., Halbach, P., 1995. Sequential leaching of marine ferromanganese precipitates: Genetic implications. *Geochim. Cosmochim. Acta* 59, 5113–5132. [https://doi.org/10.1016/0016-7037\(95\)00358-4](https://doi.org/10.1016/0016-7037(95)00358-4)

Koschinsky, A., Hein, J.R., 2003. Uptake of elements from seawater by ferromanganese crusts: Solid-phase associations and seawater speciation. *Mar. Geol.* 198, 331–351. [https://doi.org/10.1016/S0025-3227\(03\)00122-1](https://doi.org/10.1016/S0025-3227(03)00122-1)

Kuhn, T., Bau, M., Blum, N., Halbach, P., 1998. Origin of negative Ce anomalies in mixed hydrothermal-hydrogenetic Fe-Mn crusts from the Central Indian Ridge. *Earth Planet. Sci. Lett.* 163, 207–220. [https://doi.org/10.1016/S0012-821X\(98\)00188-5](https://doi.org/10.1016/S0012-821X(98)00188-5)

Kumar, M.D., Li, Y.H., 1996. Spreading of water masses and regeneration of silica and ²²⁶Ra in the Indian Ocean. *Deep. Res. Part II Top. Stud. Oceanogr.* 43, 83–110. [https://doi.org/10.1016/0967-0645\(95\)00084-4](https://doi.org/10.1016/0967-0645(95)00084-4)

Lang, S.Q., 2018. Hydrothermal stamp on the oceans. *Nat. Geosci.* 11, 10–12. <https://doi.org/10.1038/s41561-017-0044-x>

Marino, E., González, F.J., Kuhn, T., Madureira, P., Wegorzewski, A. V., Mirao, J., Medialdea, T., Oeser, M., Miguel, C., Reyes, J., Somoza, L., Lunar, R., 2019. Hydrogenetic, diagenetic and hydrothermal processes forming ferromanganese crusts in the canary island seamounts and their influence in the metal recovery rate with hydrometallurgical methods. *Minerals* 9, 439. <https://doi.org/10.3390/min9070439>

Marino, E., González, F.J., Lunar, R., Reyes, J., Medialdea, T., Castillo-Carrión, M., Bellido, E., Somoza, L., 2018. High-resolution analysis of critical minerals and elements in Fe–Mn crusts from the canary island seamount province (Atlantic ocean). *Minerals* 8, 285. <https://doi.org/10.3390/min8070285>

- Marino, E., González, F.J., Somoza, L., Lunar, R., Ortega, L., Vázquez, J.T., Reyes, J., Bellido, E., 2017. Strategic and rare elements in Cretaceous-Cenozoic cobalt-rich ferromanganese crusts from seamounts in the Canary Island Seamount Province (northeastern tropical Atlantic). *Ore Geol. Rev.* 87, 41–61. <https://doi.org/10.1016/j.oregeorev.2016.10.005>
- McLennan, S.M., 1989. Rare Earth Elements in sedimentary rocks: Influence of provenance and sedimentary processes, in: *Geochemistry and Mineralogy of Rare Earth Elements*. pp. 169–200.
- Michard, A., 1989. Rare earth element systematics in hydrothermal fluids. *Geochim. Cosmochim. Acta* 53, 745–750. [https://doi.org/10.1016/0016-7037\(89\)90017-3](https://doi.org/10.1016/0016-7037(89)90017-3)
- Mikhailik, P.E., Mikhailik, E. V., Zarubina, N. V., Blokhin, M.G., 2017. Distribution of rare-earth elements and yttrium in hydrothermal sedimentary ferromanganese crusts of the Sea of Japan (from phase analysis results). *Russ. Geol. Geophys.* 58, 1530–1542. <https://doi.org/10.1016/j.rgg.2017.11.013>
- Mills, R. A., Wells, D.M., Roberts, S., 2001. Genesis of ferromanganese crusts from the TAG hydrothermal fields. *Chem. Geol.* 176, 283–293. [https://doi.org/10.1016/S0009-2541\(00\)00404-6](https://doi.org/10.1016/S0009-2541(00)00404-6)
- Mitra, A., Elderfield, H., Greaves, M.J., 1994. Rare earth elements in submarine hydrothermal fluids and plumes from the Mid-Atlantic Ridge. *Mar. Chem.* 46, 217–235. [https://doi.org/10.1016/0304-4203\(94\)90079-5](https://doi.org/10.1016/0304-4203(94)90079-5)
- Murton, B.J., Baker, E.T., Sands, C.M., German, C.R., 2006. Detection of an unusually large hydrothermal event plume above the slow-spreading Carlsberg Ridge: NW Indian Ocean. *Geophys. Res. Lett.* 33. <https://doi.org/10.1029/2006GL026048>
- Nath, B.N., Balaram, V., Sudhakar, M., Plijger, W.L., Nagender Nath, B., Balaram, V., Sudhakar, M., Plüger, W.L., Nath, B.N., Balaram, V., Sudhakar, M., Plijger, W.L., 1992. Rare earth element geochemistry of ferromanganese deposits from the Indian Ocean. *Mar. Chem.* 38, 185–208. [https://doi.org/10.1016/0304-4203\(92\)90034-8](https://doi.org/10.1016/0304-4203(92)90034-8)
- Nath, B.N., Plüger, W.L., Roelandts, I., 1997. Geochemical constraints on the hydrothermal origin of ferromanganese encrustations from the Rodriguez Triple Junction, Indian Ocean. *Geol. Soc. London, Spec. Publ.* 119, 199–211. <https://doi.org/10.1144/gsl.sp.1997.119.01.13>
- Nishioka, J., Obata, H., Tsumune, D., 2013. Evidence of an extensive spread of hydrothermal dissolved iron in the Indian Ocean. *Earth Planet. Sci. Lett.* 361, 26–33. <https://doi.org/10.1016/j.epsl.2012.11.040>
- Noble, A.E., Lamborg, C.H., Ohnemus, D.C., Lam, P.J., Goepfert, T.J., Measures, C.I., Frame, C.H., Casciotti, K.L., DiTullio, G.R., Jennings, J., Saito, M.A., 2012. Basin-scale inputs of cobalt, iron, and manganese from the Benguela-Angola front to the South Atlantic Ocean. *Limnol. Oceanogr.* 57, 989–1010. <https://doi.org/10.4319/lo.2012.57.4.0989>
- Paropkari, A.L., Ray, D., Balaram, V., Surya Prakash, L., Mirza, I.H., Satyanarayana, M., Gnaneshwar Rao, T., Kaisary, S., 2010. Formation of hydrothermal deposits at Kings Triple Junction, northern Lau back-arc basin, SW Pacific: The geochemical perspectives. *J. Asian Earth Sci.* 38, 121–130. <https://doi.org/10.1016/j.jseaes.2009.12.003>
- Pavia, F.J., Anderson, R.F., Black, E.E., Kipp, L.E., Vivancos, S.M., Fleisher, M.Q., Charette, M.A.,

- Sanial, V., Moore, W.S., Hult, M., Lu, Y., Cheng, H., Zhang, P., Edwards, R.L., 2019. Timescales of hydrothermal scavenging in the South Pacific Ocean from 234 Th, 230 Th, and 228 Th. *Earth Planet. Sci. Lett.* 506, 146–156. <https://doi.org/10.1016/j.epsl.2018.10.038>
- Ray, D., Babu, E.V.S.S.K., Prakash, L.S., 2017. Nature of suspended particles in hydrothermal plume at 3°40'N Carlsberg Ridge: A comparison with deep oceanic suspended matter. *Curr. Sci.* 112, 139–146. <https://doi.org/10.18520/cs/v112/i01/139-146>
- Ray, D., Kamesh Raju, K.A., Baker, E.T., Srinivas Rao, A., Mudholkar, A. V., Lupton, J.E., Surya Prakash, L., Gawas, R.B., Vijaya Kumar, T., 2012. Hydrothermal plumes over the Carlsberg Ridge, Indian Ocean. *Geochemistry, Geophys. Geosystems* 13, Q01009. <https://doi.org/10.1029/2011GC003888>
- Ray, D., Mirza, I.H., Surya Prakash, L., Kaisary, S., Sarma, Y.V.B.B., Rao, B.R., Somayajulu, Y.K., Drolia, R.K., Kamesh Raju, K.A., 2008. Water-column geochemical anomalies associated with the remnants of a mega plume: A case study after CR-2003 hydrothermal event in Carlsberg Ridge, NW Indian Ocean. *Curr. Sci.* 95, 355-360.
- Ren, Y., Sun, X., Guan, Y., Xiao, Z., Liu, Y., Liao, J., Guo, Z., 2018. Distribution of Rare Earth Elements plus Yttrium among Major Mineral Phases of Marine Fe–Mn Crusts from the South China Sea and Western Pacific Ocean: A Comparative Study. *Minerals* 9, 8. <https://doi.org/10.3390/min9010008>
- Resing, J.A., Sedwick, P.N., German, C.R., Jenkins, W.J., Moffett, J.W., Sohst, B.M., Tagliabue, A., 2015. Basin-scale transport of hydrothermal dissolved metals across the South Pacific Ocean. *Nature* 523, 200–203. <https://doi.org/10.1038/nature14577>
- Sander, S.G., Koschinsky, A., 2011. Metal flux from hydrothermal vents increased by organic complexation. *Nat. Geosci.* 4, 145–150. <https://doi.org/10.1038/ngeo1088>
- Sherrell, R.M., Field, M.P., Ravizza, G., 1999. Uptake and fractionation of rare earth elements on hydrothermal plume particles at 9°45'N, East Pacific Rise. *Geochim. Cosmochim. Acta* 63, 1709–1722. [https://doi.org/10.1016/S0016-7037\(99\)00182-9](https://doi.org/10.1016/S0016-7037(99)00182-9)
- Small, C., Cochran, J.R., Sempéré, J.C., Christie, D., 1999. The structure and segmentation of the Southeast Indian Ridge. *Mar. Geol.* 161, 1–12. [https://doi.org/10.1016/S0025-3227\(99\)00051-1](https://doi.org/10.1016/S0025-3227(99)00051-1)
- Srinivasan, A., Top, Z., Schlosser, P., Hohmann, R., Iskandarani, M., Olson, D.B., Lupton, J.E., Jenkins, W.J., 2004. Mantle 3He distribution and deep circulation in the Indian Ocean. *J. Geophys. Res. C Ocean.* 109, C06012. <https://doi.org/10.1029/2003JC002028>
- Stumm W. and Morgan J. J., 1981. An Introduction Emphasizing Chemical Equilibria in Natural Waters, in: *Aquatic Chemistry*.
- Sun, J., Zhou, Y., Chen, C., Kwan, Y.H., Sun, Y., Wang, X., Yang, L., Zhang, R., Wei, T., Yang, Y., Qu, L., Sun, C., Qian, P.-Y., 2020. Nearest vent, dearest friend: biodiversity of Tiancheng vent field reveals cross-ridge similarities in the Indian Ocean. *R. Soc. Open Sci.* 7. <https://doi.org/10.1098/rsos.200110>
- Surya Prakash, L., Ray, D., Paropkari, A.L., Mudholkar, A. V., Satyanarayanan, M., Sreenivas, B., Chandrasekharam, D., Kota, D., Kamesh Raju, K.A., Kaisary, S., Balaram, V., Gurav, T., 2012. Distribution of REEs and yttrium among major geochemical phases of marine Fe-Mn-oxides:

Comparative study between hydrogenous and hydrothermal deposits. *Chem. Geol.* 312–313, 127–137. <https://doi.org/10.1016/j.chemgeo.2012.03.024>

Takahashi, Y., Manceau, A., Geoffroy, N., Marcus, M.A., Usui, A., 2007. Chemical and structural control of the partitioning of Co, Ce, and Pb in marine ferromanganese oxides. *Geochim. Cosmochim. Acta* 71, 984–1008. <https://doi.org/10.1016/j.gca.2006.11.016>

Takahata, N., Shirai, K., Ohmori, K., Obata, H., Gamo, T., Sano, Y., 2018. Distribution of helium-3 plumes and deep-sea circulation in the central Indian Ocean. *Terr. Atmos. Ocean. Sci.* 29, 331–340. <https://doi.org/10.3319/tao.2017.10.21.02>

Thi Dieu Vu, H., Sohrin, Y., 2013. Diverse stoichiometry of dissolved trace metals in the Indian Ocean. *Sci. Rep.* 3, 1745. <https://doi.org/10.1038/srep01745>

Toner, B.M., Fakra, S.C., Manganini, S.J., Santelli, C.M., Marcus, M.A., Moffett, J.W., Rouxel, O., German, C.R., Edwards, K.J., 2009. Preservation of iron(II) by carbon-rich matrices in a hydrothermal plume. *Nat. Geosci.* 2, 197–201. <https://doi.org/10.1038/ngeo433>

Toth, J.R., 1980. Deposition of submarine crusts rich in manganese and iron. *Geol. Soc. Am. Bull.* 91, 44–54. [https://doi.org/10.1130/0016-7606\(1980\)91<44:DOSCRI>2.0.CO](https://doi.org/10.1130/0016-7606(1980)91<44:DOSCRI>2.0.CO)

Usui, A., Nishimura, A., 1992. Submersible observations of hydrothermal manganese deposits on the Kaikata Seamount, Izu-Ogasawara (Bonin) Arc. *Mar. Geol.* 106, 203–216. [https://doi.org/10.1016/0025-3227\(92\)90130-A](https://doi.org/10.1016/0025-3227(92)90130-A)

Valk, O., Rutgers van der Loeff, M.M., Geibert, W., Gdaniec, S., Rijkenberg, M.J.A., Moran, S.B., Lepore, K., Edwards, R.L., Lu, Y., Puigcorb , V., 2018. Importance of Hydrothermal Vents in Scavenging Removal of ²³⁰Th in the Nansen Basin. *Geophys. Res. Lett.* 45, 10539–10548. <https://doi.org/10.1029/2018GL079829>

Wilson, D.J., Piotrowski, A.M., Galy, A., McCave, I.N., 2012. A boundary exchange influence on deglacial neodymium isotope records from the deep western Indian Ocean. *Earth Planet. Sci. Lett.* 341, 35–47. <https://doi.org/10.1016/j.epsl.2012.06.009>

Wu, J., Wells, M.L., Rember, R., 2011. Dissolved iron anomaly in the deep tropical-subtropical Pacific: Evidence for long-range transport of hydrothermal iron. *Geochim. Cosmochim. Acta* 75, 460–468. <https://doi.org/10.1016/j.gca.2010.10.024>

Y cel, M., Gartman, A., Chan, C.S., Luther, G.W., 2011. Hydrothermal vents as a kinetically stable source of iron-sulphide-bearing nanoparticles to the ocean. *Nat. Geosci.* 4, 367–371. <https://doi.org/10.1038/ngeo1148>

Figure Legends

Figure 1: Study area showing the Indian mid-ocean ridges (Carlsberg, Central Indian, Southwest and Southeast Indian Ridges), Central Indian Ocean Basin and Andaman Sea. White squares represent sample locations, yellow circles indicate unidentified/inferred active hydrothermal venting, red and green circles are known active and inactive hydrothermal fields (Beaulieu et al., 2013).

Figure 2: Ternary diagrams of (A) Fe-Mn-(Co+Ni+Zn)x10, (B) Fe-Mn-(Co+Ni+Cu)x10, (C) Fe-Mn-(Co)x10 and (D) (Zr+Y+Ce)x100- (Cu+Ni)x10-(Fe+Mn)/4 (Toth, 1980; Usui and Nishimura, 1992; Frank et al., 2006; Josso et al., 2017) to classify the genetic origin of ferromanganese crusts from Indian mid-oceanic ridges.

Figure 3: PAAS normalized rare earth element pattern of ferromanganese crusts from Carlsberg Ridge (A & B), Central Indian Ridge (C & D) and South West Indian Ridge (E & F).

Figure 4: Modified REE discrimination plots (A) Ce_{SN}/Ce_{SN}^* vs Nd and (B) Ce_{SN}/Ce_{SN}^* vs Y_{SN}/Ho_{SN} of ferromanganese crusts from Indian mid-oceanic ridges to effectively discriminate between different genetic types.

Figure 5: Ce_{xs}/Ce_{bulk} versus Ce_{bulk} plot (Kuhn et al., 1998) of ferromanganese crusts from Indian mid-oceanic ridges to understand the influence of hydrothermal activity/plume. Several different sample sets from previous studies including crusts of hydrogenous origin (Andaman Sea and CIOB from Surya Prakash et al., 2012; Central Indian Ocean Basin Kalangutkar et al., 2015; Pacific Ocean-Bau et al., 1996) and hydrothermal origin (Lau Basin from Paropkari et al., 2010, Andaman Sea from Surya Prakash et al., 2012, hydrothermal plume particles and crusts from TAG from German et al., 1990; R. A. Mills et al., 2001; (Bau et al., 2014) and mixed hydrogenous and hydrothermal crusts (CIR from Kuhn et al., 1998; Nath et al., 1997 ; CIOB from Kalangutkar et al., 2015 and Northwest Pacific from Mills et al., 2001) have been plotted for Ce_{xs}/Ce_{bulk} versus Ce_{bulk} .

Figure 6: Rare Earth Elements and Yttrium (REE-Y) abundances in major geochemical phases of Fe-Mn crusts collected from (A) CR, (B) CIR, (C) SWIR. For comparison, hydrogenous crusts (D & E) from seamount (SM2), Andaman Sea, Central Indian Ocean Basin and hydrothermal crusts (F) from submarine volcano (CSM), Andaman Sea (Kamesh Raju et al., 2012a; Surya Prakash et al., 2012) are shown.

Figure 7: PAAS normalized rare earth element pattern of bulk and major geochemical fractions of Fe-Mn-crusts from Carlsberg Ridge (CR-A & B), Central Indian Ridge (CIR-C) and Southwest Indian Ridge (SWIR-D & E). For comparison, hydrogenous crusts (F & G) from seamount (SM2), Andaman Sea, Central Indian Ocean Basin and hydrothermal crusts (H) from submarine volcano (CSM), Andaman Sea (Kamesh Raju et al., 2012a; Surya Prakash et al., 2012) are shown.

Figure 8: Illustration of formation mechanism for hydrogenous and mixed origin (hydrothermal/hydrogenous) ferromanganese crusts from mid-oceanic ridges of Indian Ocean.

Figures:

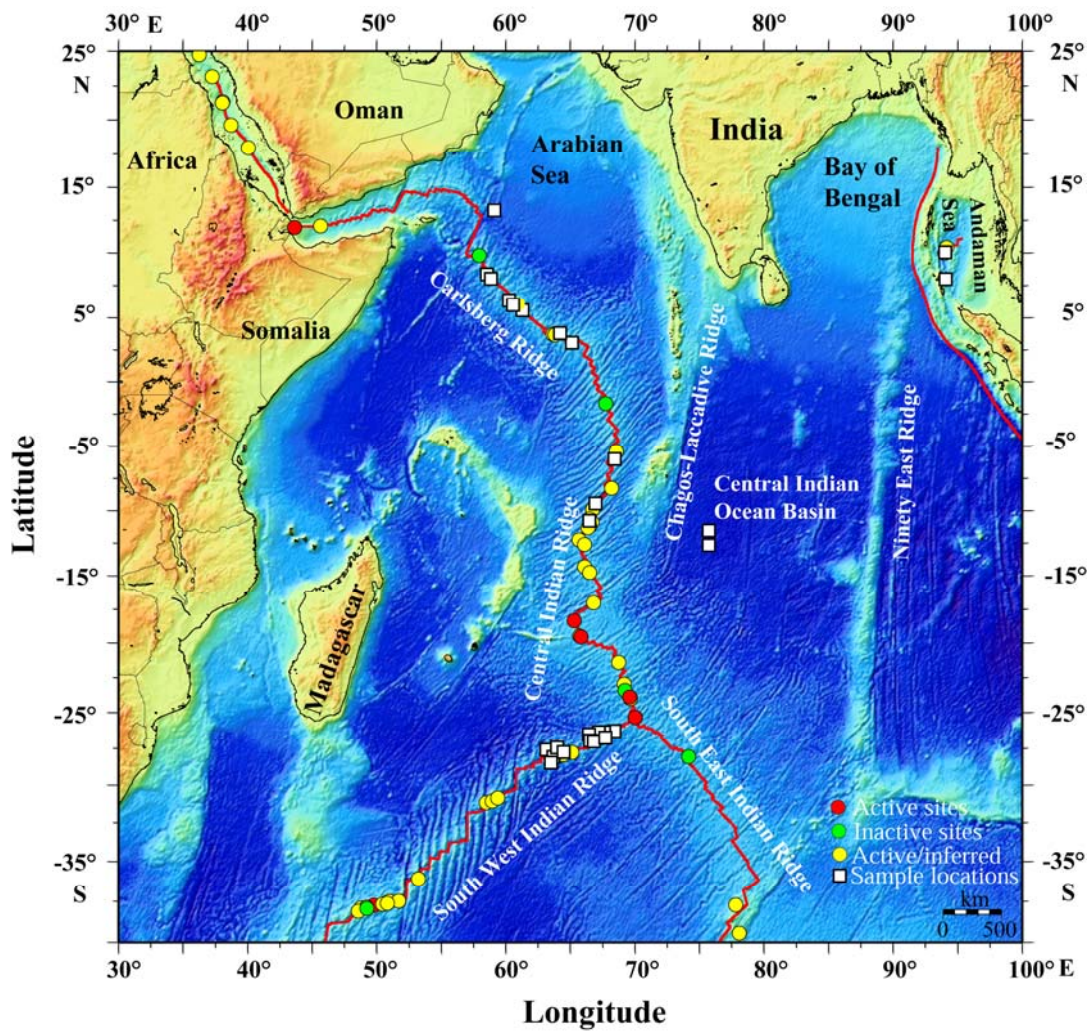


Figure 1.

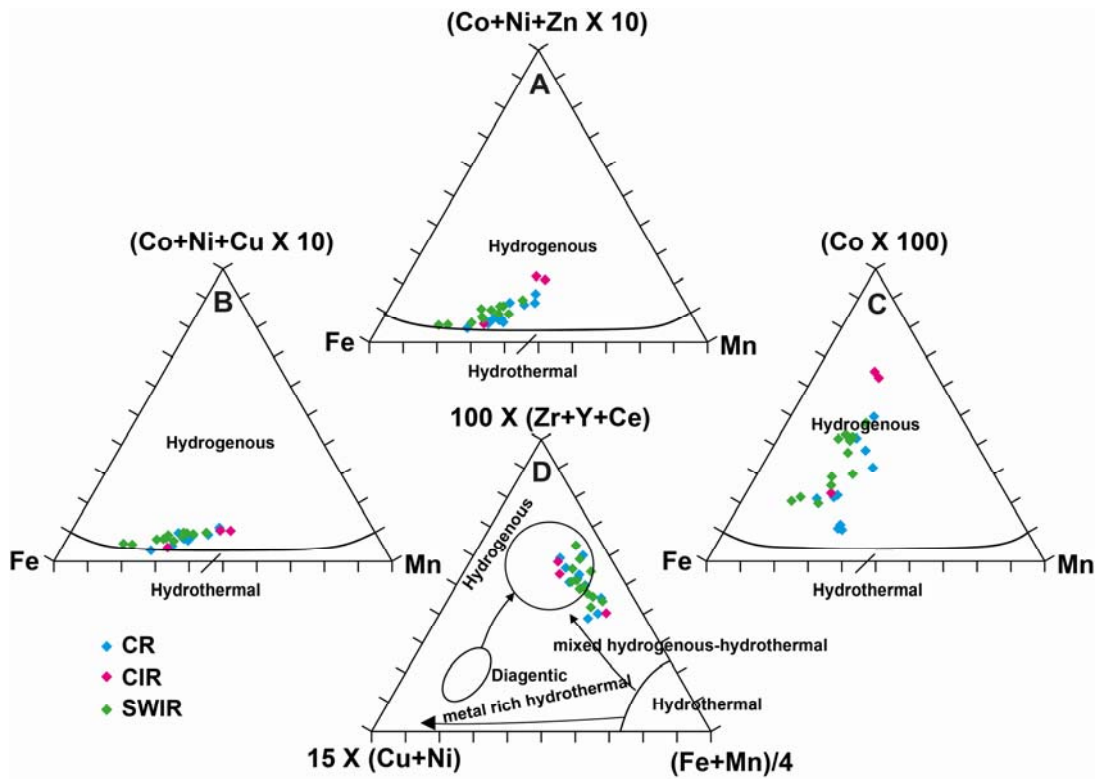


Figure 2.

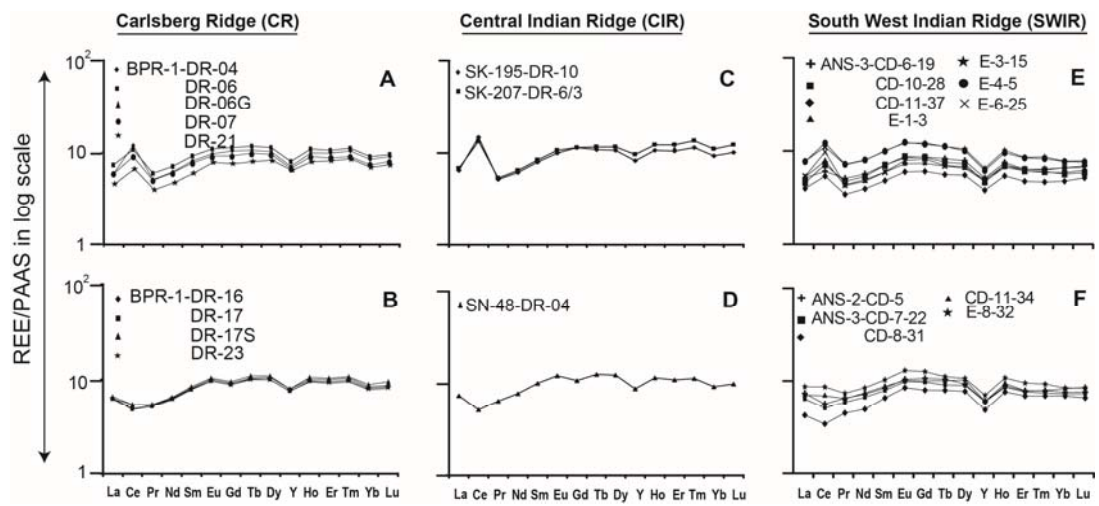


Figure 3.

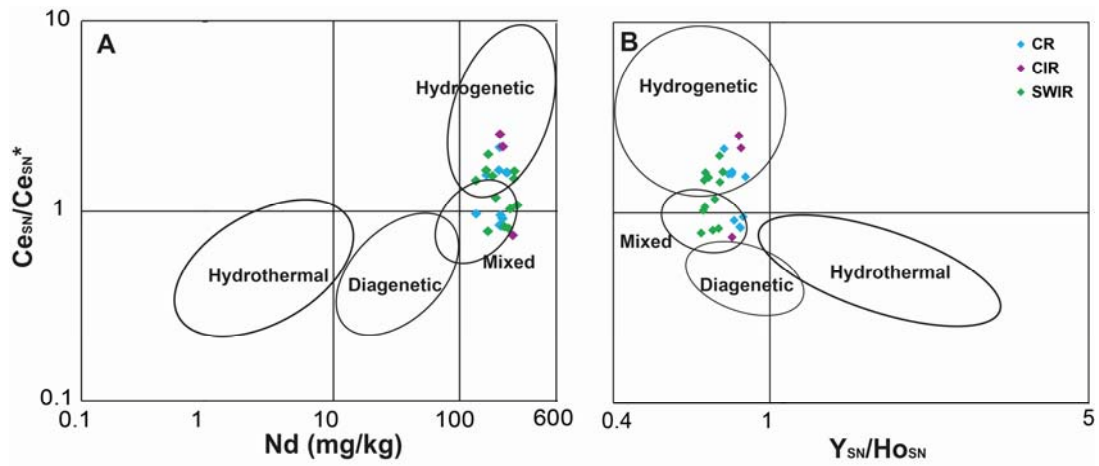


Figure 4.

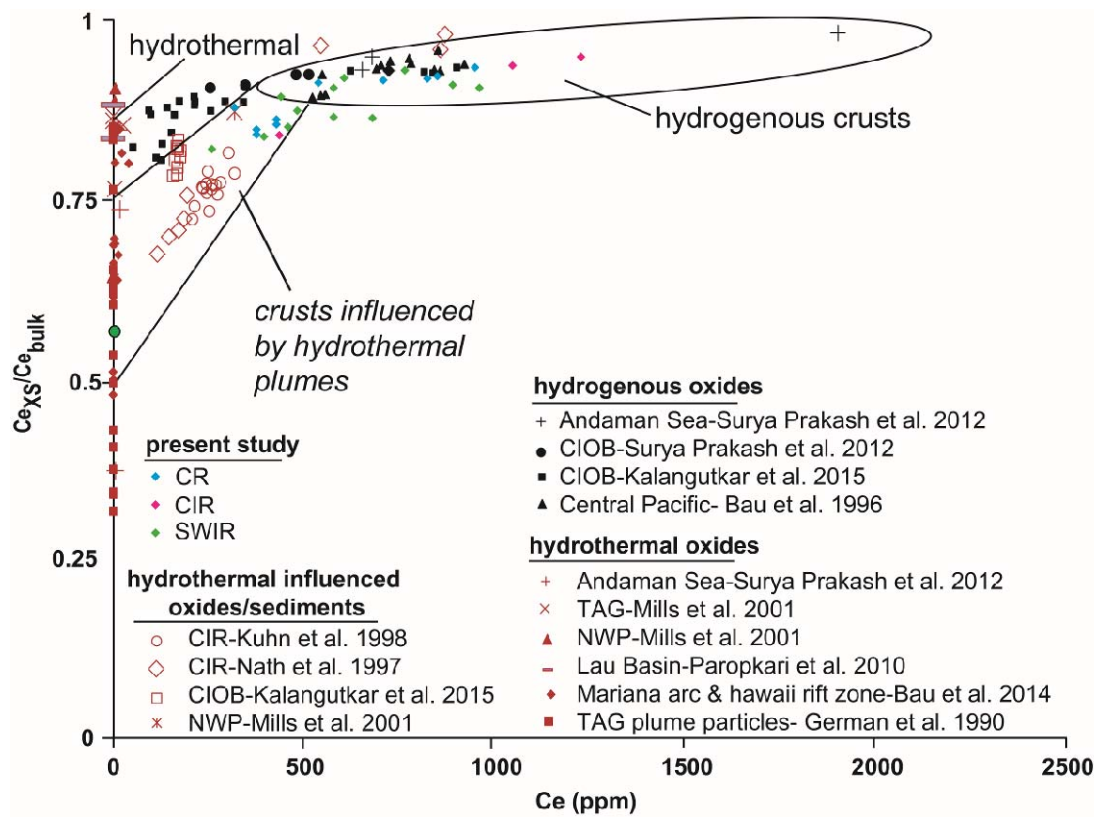


Figure 5.

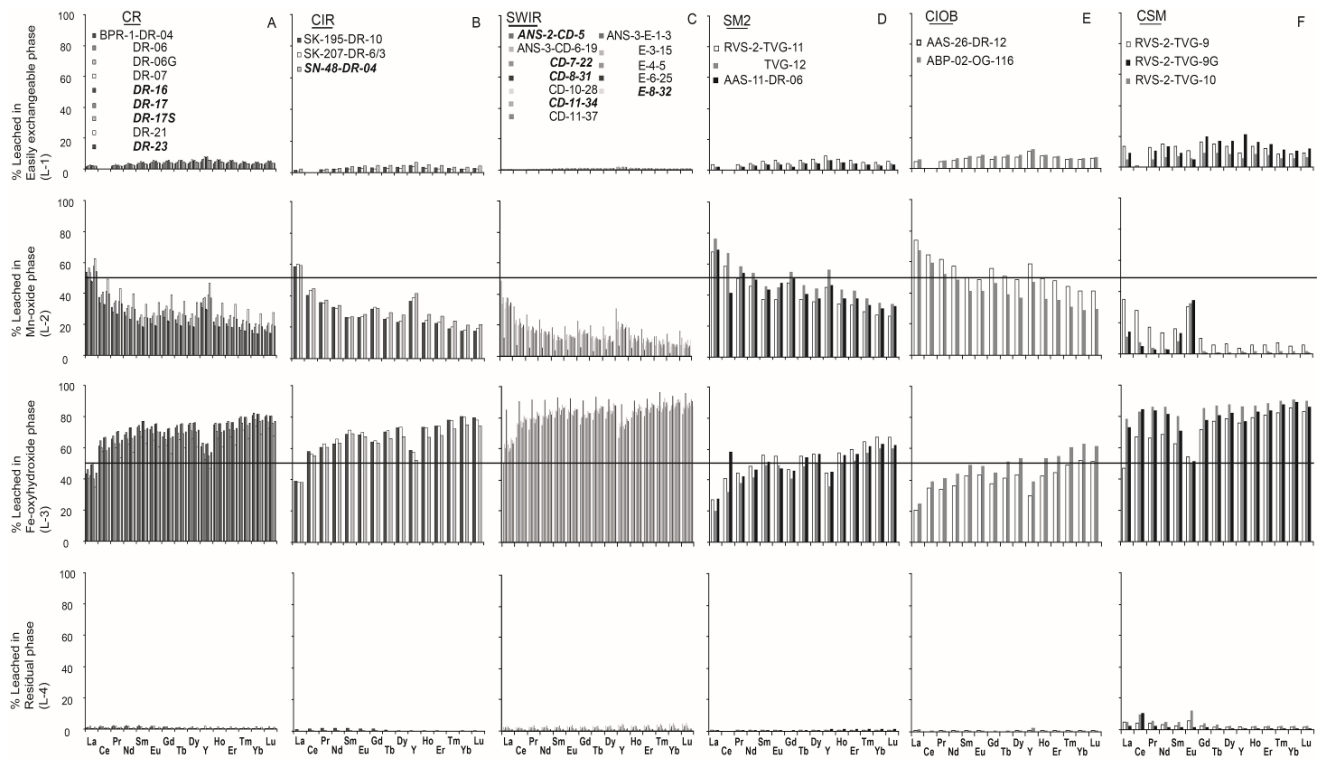


Figure 6.

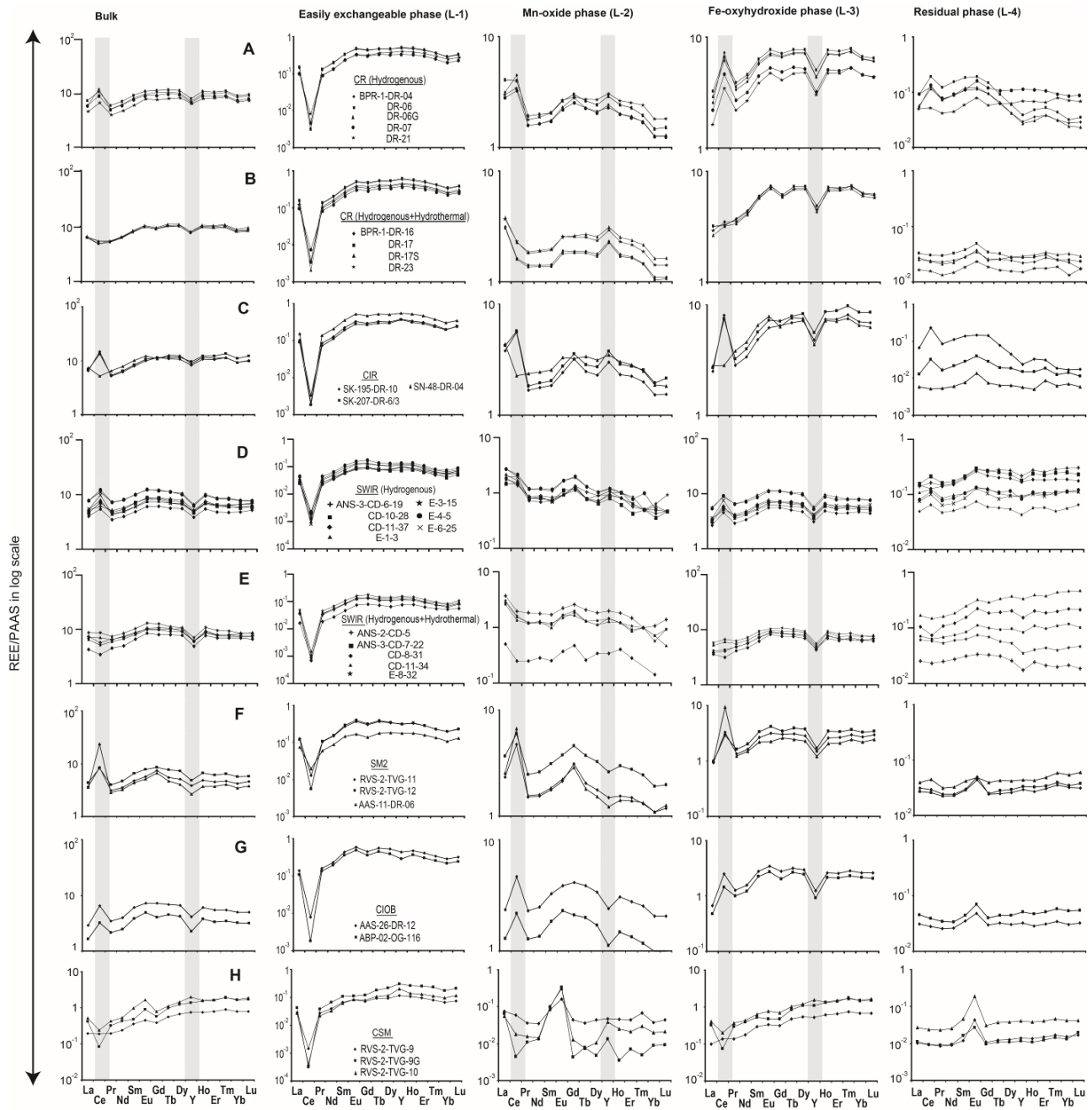


Figure 7.

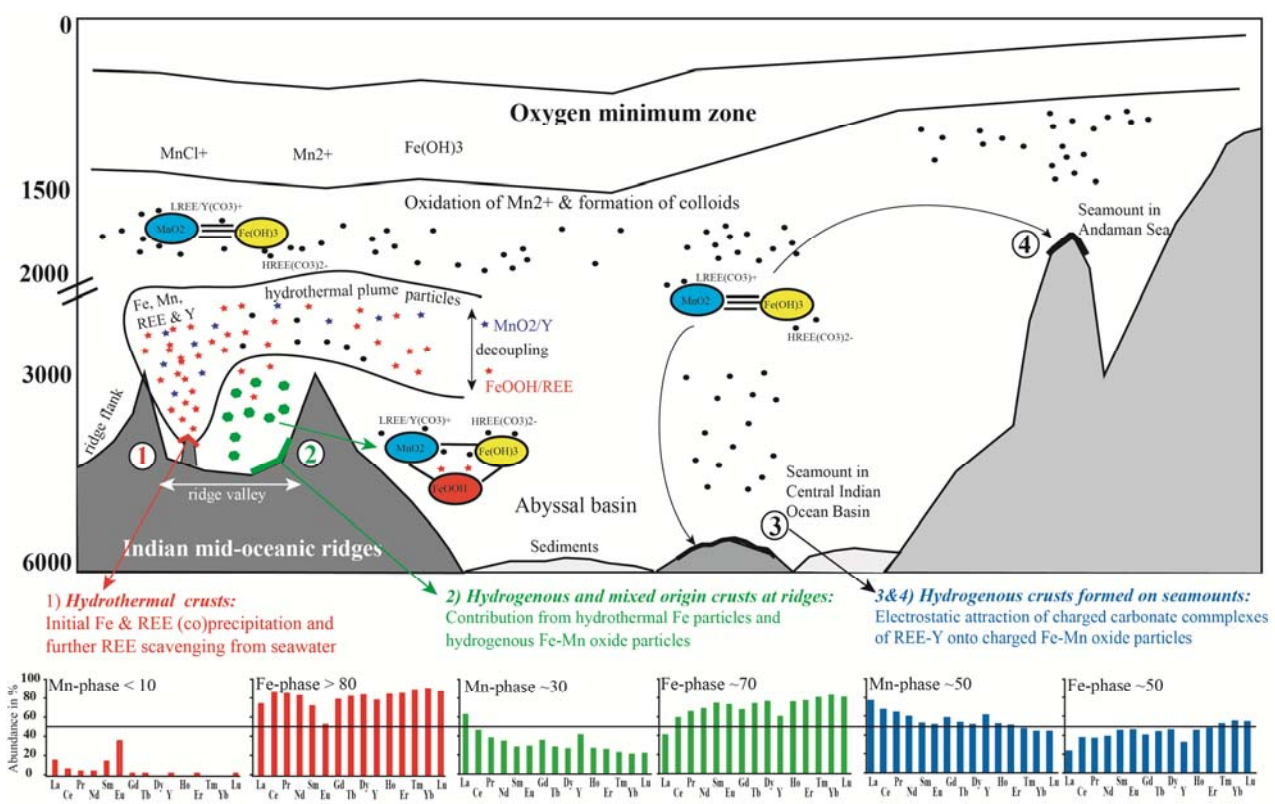


Figure 8.

Table 1: Concentrations (in wt%) of Fe, Mn, Co, Ni, Cu and Zn in ferromanganese crusts from Carlsberg Ridge (CR), Central Indian Ridge (CIR) and Southwest Indian Ridge (SWIR) along with sampling locations and water depths (m).

| Ridge | Sample Id | Latitude | Longitude | Depth (m) | Fe | Mn | Co | Ni | Cu | Zn | Origin |
|----------------|------------|--------------|-------------|-----------|-------|-------|-------|--------|-------|-------|--------|
| Carls | DR-04 | 13°16.67'N | 59° 16.25'E | 3565 | 16.7 | 15.8 | 0.139 | 0.277 | 0.040 | 0.072 | HG |
| | DR-06 | 08°15.66'N | 58° 30.91'E | 2519 | 17.4 | 14.2 | 0.302 | 0.285 | 0.020 | 0.060 | HG |
| | DR-6G | -do- | -do- | -do- | 16.7 | 13.3 | 0.208 | 0.218 | 0.018 | 0.045 | HG |
| | DR-07 | 08°03.82'N | 58° 50.94'E | 3382 | 15.3 | 12.6 | 0.190 | 0.241 | 0.023 | 0.051 | HG |
| | DR-16 | 06°19.08'N | 60° 30.51'E | 3096 | 18.1 | 12.4 | 0.035 | 0.148 | 0.026 | 0.050 | HG+HT |
| | DR-17 | 06°07.33'N | 60° 45.27'E | 2853 | 16.2 | 12.5 | 0.038 | 0.180 | 0.024 | 0.050 | HG+HT |
| | DR-17S | -do- | -do- | -do- | 17.3 | 12.5 | 0.044 | 0.197 | 0.022 | 0.055 | HG+HT |
| | DR-21 | 03°39.94'N | 63° 45.62'E | 3244 | 21.6 | 7.96 | 0.082 | 0.046 | 0.023 | 0.050 | HG |
| DR-23 | 03°39.71'N | 63° 49.92'E | 2312 | 21.8 | 10.7 | 0.090 | 0.106 | 0.0195 | 0.052 | HG+HT | |
| Centr India | DR-10 | 06° 03.04'S | 68° 29.86'E | 2362 | 15.7 | 15.2 | 0.576 | 0.305 | 0.019 | 0.048 | HG |
| | DR-6/3 | 09° 27.40'S | 66° 58.24'E | 1735 | 14.9 | 16.5 | 0.535 | 0.294 | 0.026 | 0.052 | HG |
| | DR-04 | 10°47.62'S | 66° 30.27'E | 2741 | 22.1 | 10.8 | 0.101 | 0.082 | 0.037 | 0.045 | HG+HT |
| South India | CD-5 | 26° 36.22' S | 67°19.38'E | 2829 | 19.1 | 12.9 | 0.137 | 0.145 | 0.061 | 0.130 | HG+HT |
| | CD6-19 | 27°05.01' S | 66° 53.15'E | 3040 | 26.2 | 7.19 | 0.095 | 0.056 | 0.062 | 0.087 | HG |
| | CD7-22 | 26° 23.45'S | 67° 43.12'E | 3039 | 20.8 | 9.89 | 0.108 | 0.092 | 0.071 | 0.144 | HG+HT |
| | CD8-31 | 26° 21.88'S | 68° 18.16'E | 3426 | 21.8 | 8.83 | 0.076 | 0.093 | 0.049 | 0.110 | HG+HT |
| | CD10-28 | 27° 03.60'S | 67° 13.76'E | 3708 | 25.8 | 5.92 | 0.083 | 0.048 | 0.066 | 0.094 | HG |
| | CD11-34 | 26°44.98'S | 66° 31.40'E | 2482 | 24.6 | 11.03 | 0.259 | 0.138 | 0.060 | 0.103 | HG+HT |
| | CD11-37 | 27° 00.52'S | 66° 30.01'E | 3020 | 19.4 | 9.02 | 0.117 | 0.090 | 0.064 | 0.099 | HG |
| | E-1-3 | 27° 33.77'S | 63° 56.56'E | 2670 | 17.5 | 10.81 | 0.211 | 0.127 | 0.062 | 0.119 | HG |
| | E-3-15 | 28° 02.98'S | 63° 42.64'E | 2965 | 20.2 | 11.83 | 0.191 | 0.117 | 0.037 | 0.155 | HG |
| | E-4-5 | 27° 42.96'S | 64° 19.30'E | 2968 | 21.0 | 10.99 | 0.247 | 0.099 | 0.051 | 0.093 | HG |
| | E-6-25 | 28°23.03'S | 63° 30.16'E | 3100 | 18.7 | 11.01 | 0.211 | 0.137 | 0.069 | 0.123 | HG |
| E-8-32 | 27°36.32'S | 63° 15.71'E | 2659 | 18.0 | 14.47 | 0.294 | 0.193 | 0.059 | 0.107 | HG+HT | |

HG-hydrogenous; HT-hydrothermal

Table 2: Rare earth elements and Yttrium concentrations (in ppm) of ferromanganese crusts from Carlsberg Ridge (CR), Central Indian Ridge (CIR) and Southwest Indian Ridge (SWIR)

| Sample Id | La | Ce | Pr | Nd | Sm | Eu | Gd | Tb | Dy | Y | Ho | Er | Tm | Yb | Lu | TREE | Ce/Ce* |
|-------------------------|-----|------|-------|-----|-------|-------|-------|------|-------|-----|-------|-------|------|-------|------|------|--------|
| Carlsberg | | | | | | | | | | | | | | | | | |
| DR-04 | 223 | 951 | 45.5 | 208 | 45.0 | 10.46 | 48.6 | 8.20 | 48.0 | 191 | 9.75 | 27.8 | 4.19 | 23.6 | 3.90 | 1657 | 2.17 |
| DR-06 | 272 | 829 | 52.1 | 235 | 49.6 | 11.73 | 51.2 | 8.66 | 51.4 | 216 | 10.59 | 29.3 | 4.33 | 25.0 | 4.07 | 1634 | 1.60 |
| DR-6G | 282 | 851 | 53.0 | 240 | 50.7 | 11.76 | 52.4 | 9.00 | 53.0 | 218 | 10.84 | 30.0 | 4.51 | 25.4 | 4.13 | 1677 | 1.60 |
| DR-07 | 223 | 713 | 44.6 | 205 | 42.8 | 9.86 | 42.9 | 7.55 | 44.4 | 182 | 8.91 | 24.8 | 3.67 | 20.6 | 3.44 | 1394 | 1.64 |
| DR-16 | 243 | 387 | 46.9 | 214 | 44.8 | 10.73 | 42.0 | 7.97 | 48.8 | 212 | 9.90 | 28.1 | 4.18 | 23.4 | 3.71 | 1114 | 0.84 |
| DR-17 | 238 | 382 | 45.2 | 207 | 43.2 | 10.30 | 40.9 | 7.82 | 46.6 | 203 | 9.55 | 26.7 | 3.98 | 22.6 | 3.62 | 1088 | 0.84 |
| DR-17S | 248 | 432 | 47.8 | 218 | 46.5 | 11.03 | 43.7 | 8.33 | 50.3 | 215 | 10.39 | 29.2 | 4.31 | 24.7 | 4.05 | 1179 | 0.91 |
| DR-21 | 179 | 542 | 36.3 | 163 | 34.0 | 8.54 | 35.8 | 6.26 | 39.0 | 177 | 8.04 | 23.3 | 3.48 | 19.6 | 3.26 | 1102 | 1.55 |
| DR-23 | 236 | 431 | 45.7 | 211 | 43.7 | 10.33 | 40.7 | 7.64 | 46.2 | 202 | 9.33 | 25.8 | 3.84 | 22.0 | 3.50 | 1137 | 0.95 |
| Central Indian | | | | | | | | | | | | | | | | | |
| DR-10 | 249 | 1179 | 45.30 | 209 | 44.04 | 10.65 | 52.57 | 8.35 | 49.80 | 222 | 10.47 | 29.62 | 4.58 | 26.00 | 4.38 | 1923 | 2.54 |
| DR-6/3 | 261 | 1061 | 47.05 | 220 | 46.73 | 11.43 | 53.36 | 8.96 | 54.59 | 258 | 12.03 | 34.76 | 5.50 | 31.19 | 5.30 | 1853 | 2.19 |
| DR-04 | 281 | 411 | 57.34 | 263 | 55.55 | 13.09 | 50.14 | 9.79 | 57.59 | 235 | 11.49 | 31.48 | 4.63 | 26.25 | 4.28 | 1277 | 0.75 |
| Southwest Indian | | | | | | | | | | | | | | | | | |
| CD-5 | 281 | 448 | 57.65 | 244 | 46.60 | 11.25 | 49.65 | 8.10 | 43.50 | 162 | 8.80 | 22.30 | 3.20 | 21.35 | 3.30 | 1249 | 0.81 |
| CD6-19 | 199 | 484 | 45.15 | 193 | 39.35 | 9.15 | 40.25 | 6.40 | 36.85 | 139 | 7.45 | 18.25 | 2.60 | 18.70 | 3.00 | 1104 | 1.18 |
| CD7-22 | 245 | 405 | 51.95 | 226 | 43.90 | 10.65 | 45.25 | 7.00 | 42.00 | 162 | 8.50 | 21.75 | 3.00 | 20.40 | 3.15 | 1134 | 0.83 |
| CD8-31 | 162 | 272 | 39.55 | 167 | 36.40 | 9.15 | 37.1 | 6.15 | 36.20 | 131 | 7.55 | 19.65 | 2.80 | 19.45 | 2.85 | 818 | 0.78 |
| CD10-28 | 177 | 572 | 41.95 | 183 | 39.20 | 9.40 | 39.9 | 5.90 | 34.15 | 126 | 7.00 | 17.55 | 2.45 | 16.10 | 2.55 | 1147 | 1.53 |
| CD11-34 | 269 | 552 | 56.85 | 252 | 48.55 | 10.95 | 46.55 | 7.75 | 48.20 | 163 | 9.30 | 22.50 | 3.20 | 23.45 | 3.70 | 1354 | 1.03 |
| CD11-37 | 153 | 431 | 30.60 | 134 | 26.90 | 6.50 | 28.35 | 4.35 | 25.95 | 104 | 5.40 | 13.60 | 1.90 | 13.50 | 2.25 | 878 | 1.45 |
| E-1-3 | 202 | 626 | 37.90 | 162 | 33.15 | 7.90 | 34.45 | 5.35 | 30.85 | 129 | 6.65 | 17.60 | 2.40 | 16.65 | 2.70 | 1185 | 1.64 |
| E-3-15 | 297 | 881 | 63.10 | 270 | 55.70 | 13.10 | 56.55 | 8.60 | 49.10 | 177 | 10.05 | 24.35 | 3.50 | 21.95 | 3.40 | 1757 | 1.48 |
| E-4-5 | 295 | 965 | 63.70 | 272 | 55.00 | 13.35 | 54.85 | 8.65 | 46.85 | 168 | 9.45 | 24.00 | 3.35 | 21.75 | 3.30 | 1836 | 1.63 |
| E-6-25 | 206 | 776 | 38.75 | 168 | 33.20 | 8.55 | 38.45 | 5.40 | 31.90 | 134 | 7.00 | 18.25 | 2.55 | 18.75 | 2.90 | 1356 | 2.00 |
| E-8-32 | 332 | 688 | 65.10 | 286 | 57.10 | 14.00 | 58.75 | 8.60 | 50.00 | 189 | 10.70 | 27.10 | 3.75 | 23.80 | 3.65 | 1628 | 1.08 |